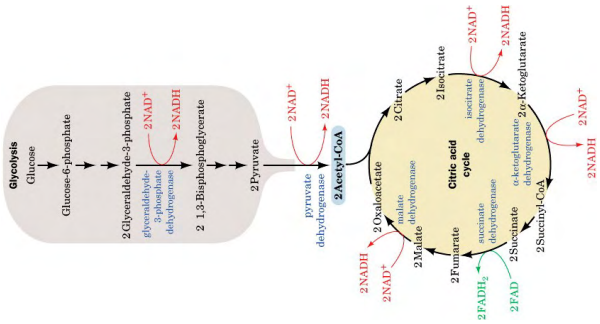

Figure 22-1 The sites of electron transfer that form NADH and $FADH_2$ in glycolysis and the citric acid cycle.

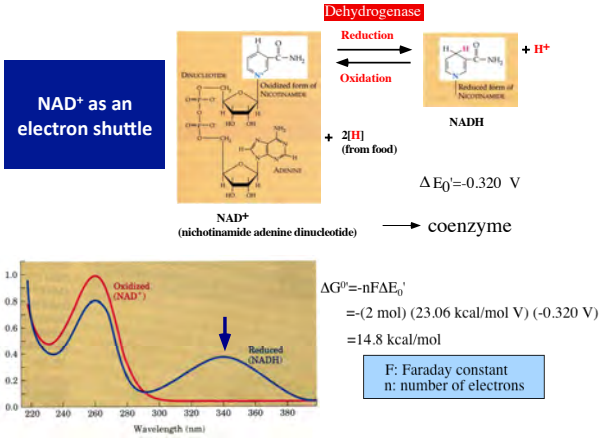

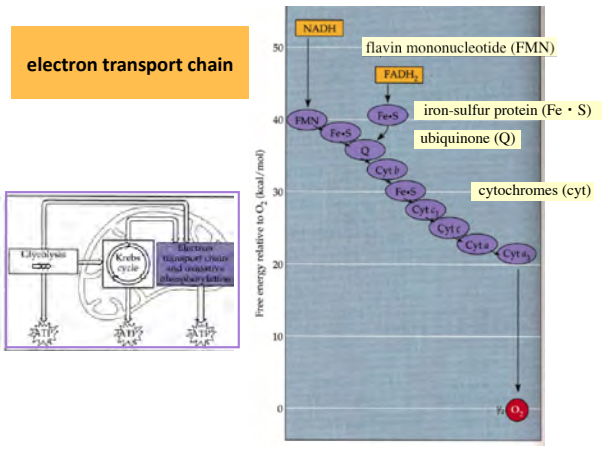

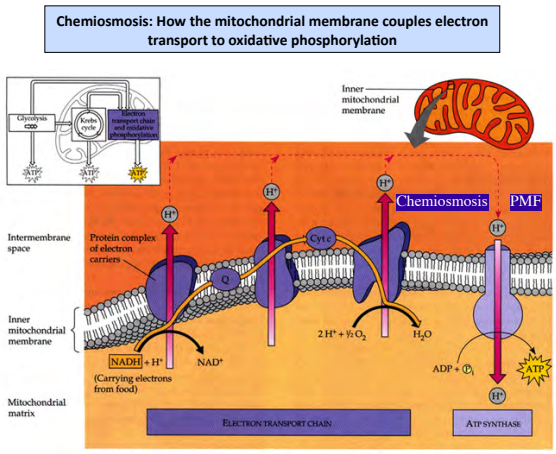

Mitochondria. (*a*) An electron micrograph of an animal mitochondrion.

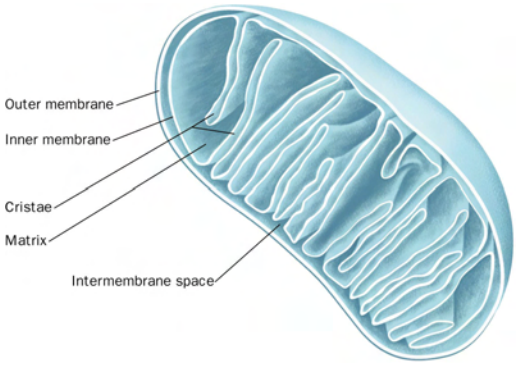

Mitochondria. (*b*) Cutaway diagram of a mitochondrion.

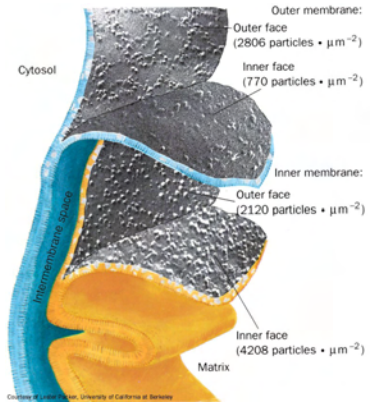

Freeze-fracture and freeze-etch electron micrographs of the inner and outer mitochondrial membranes.

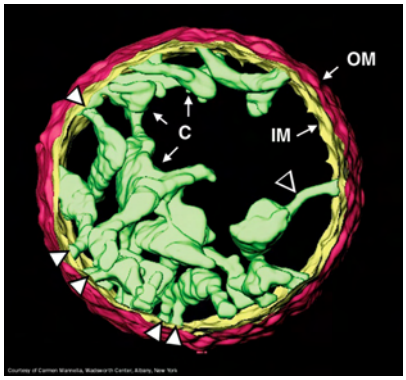

Electron microscopy–based three-dimensional image reconstruction of a rat liver mitochondrion.

The glycerophosphate shuttle.

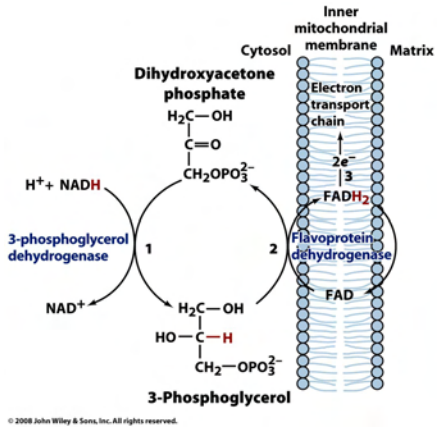

Figure 16-20

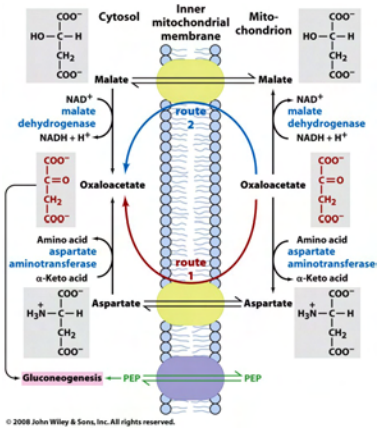

The mitochondrial electron-transport chain.

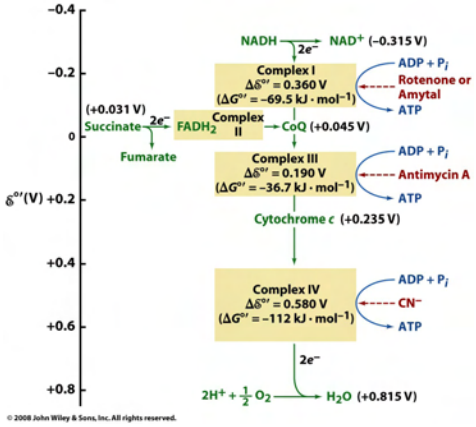

Effect of inhibitors on electron transport.

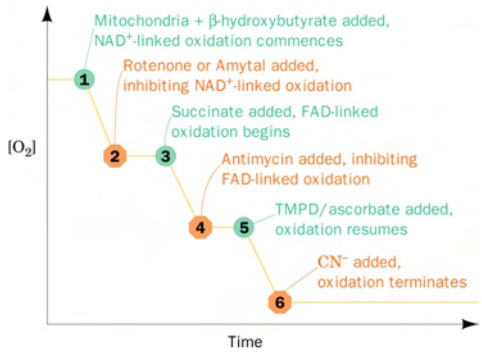

The oxygen electrode.

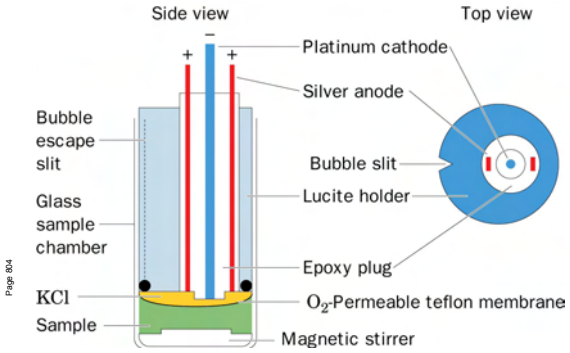

Electron micrographs of mouse liver mitochondria.

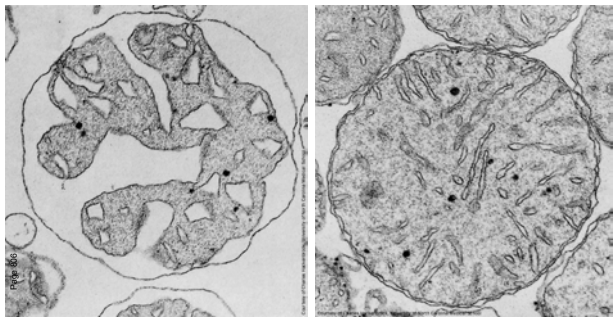

(*a*) In the actively respiring state. (*b*) In the resting state.

The mitochondrial electron-transport chain.

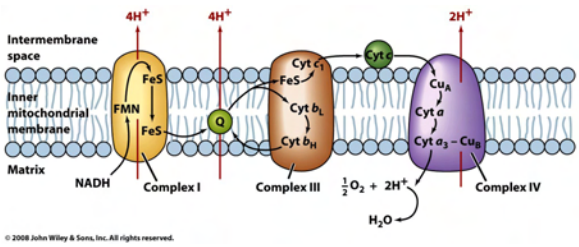

Cytochromeの電子の流れの順序

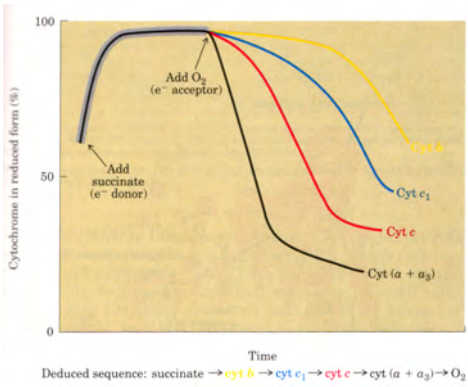

阻害剤と電子の流れ

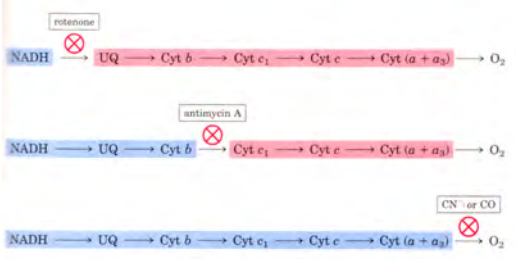

Coupling of electron transport (*green arrow*) and ATP synthesis.

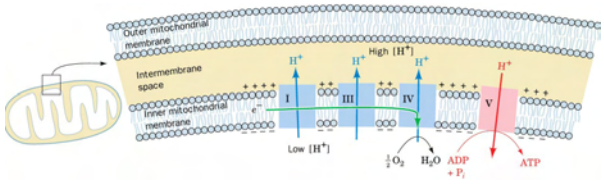

Uncoupling of oxidative phosphorylation.

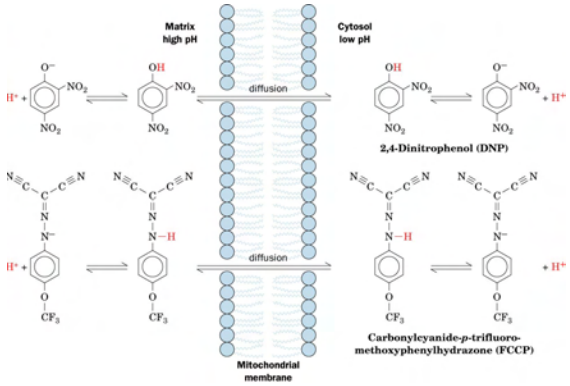

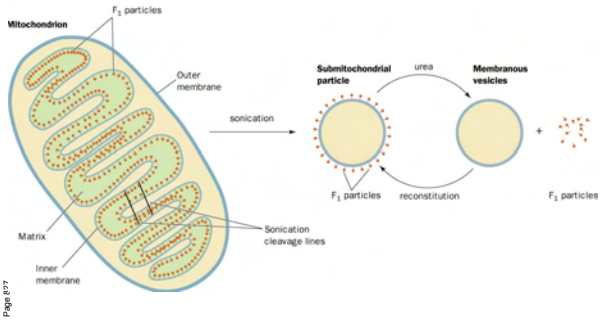

Figure 22-36 Interpretive drawings of the mitochondrial membrane at various stages of dissection.

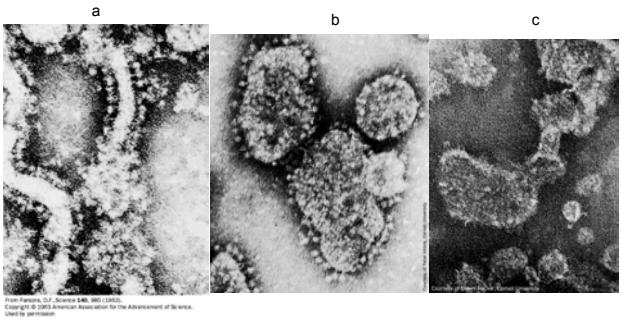

Electron micrographs of cristae from (a) intact mitochondria showing their F1 "lollipops" projecting into the matrix, (b) submitochondrial particles, showing their outwardly projecting F1 lollipops, and (c) submitochondrial particles after treatment with urea.

ATP synthase, a molecular machine (fig9-14)

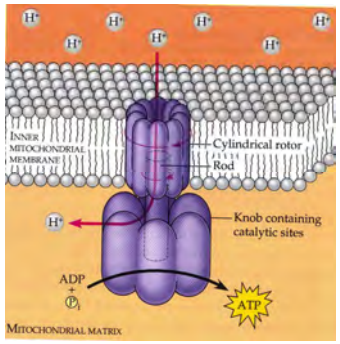

F型ATPaseモーターの構造

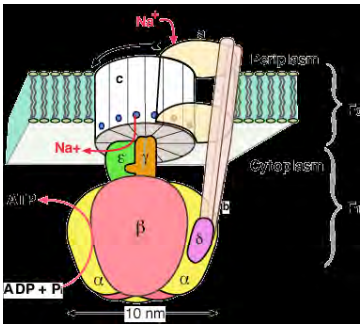

F型ATPase

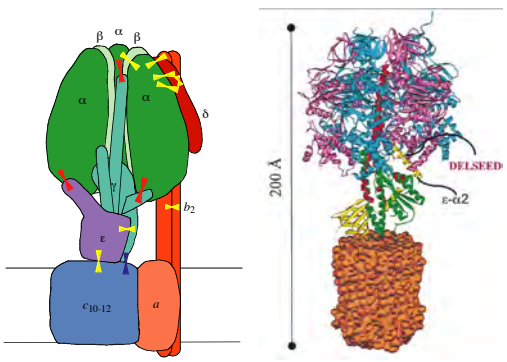

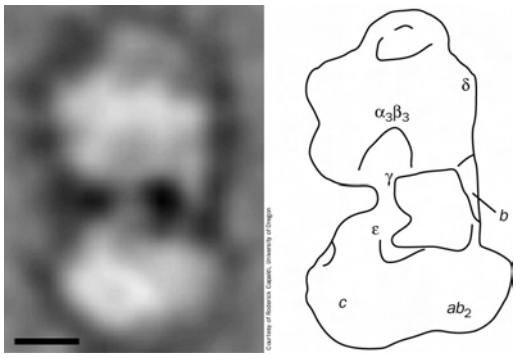

Electron microscopy–based image of *E. coli* F_1F_0–ATPase.

X-Ray structure of F_1–ATPase from bovine heart mitochondria.

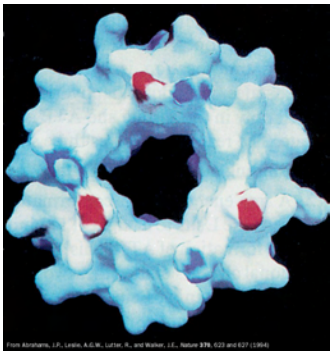

X-Ray structure of F_1–ATPase from bovine heart mitochondria.
The surface of the inner portion of the $\alpha_3\beta_3$ assembly.

The γ, δ, and ε subunits in the X-ray structure of bovine F_1–ATPase.

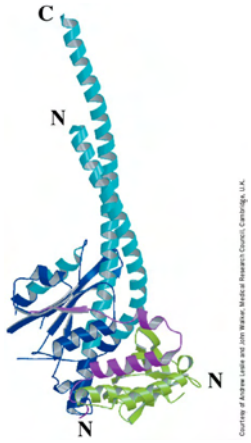

NMR structures of the *c* subunit of *E. coli* F_1F_0–ATPase.

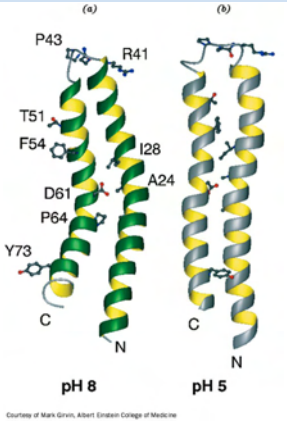

Electron density map of the yeast mitochondrial F_1– complex.

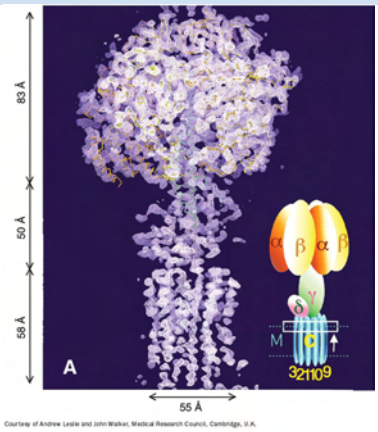

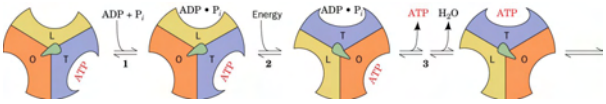

Energy-dependent binding change mechanism for ATP synthesis by proton-translocating ATP synthase.

ATPaseの構造変化と触媒活性モデル

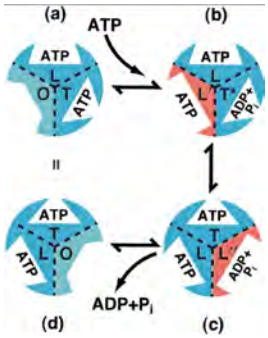

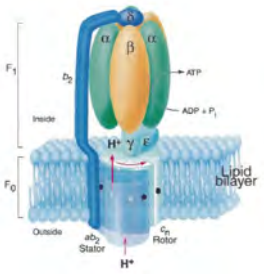

O(オープン)型：触媒不活性で基質・生成物に親和性なし
L(ルーズ)型：弱い親和性をもつが、触媒活性なし
T(タイト)型：強い親和性をもち、触媒活性をもつ

F型ATPase回転実証の実験系

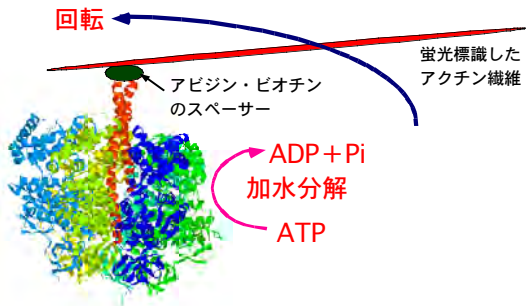

ATPaseのα　β　γ複合体

Noji et al. (1997) Nature

Rotation of the *c*-ring in *E. coli* F_1F_0–ATPase

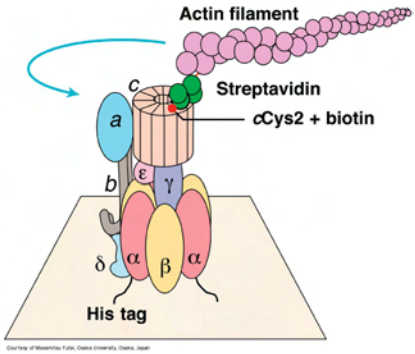

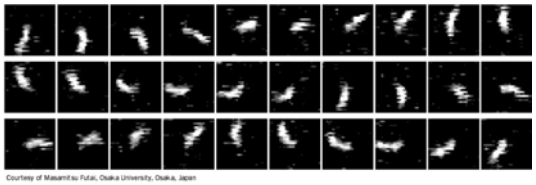

Rotation of the *c*-ring in *E. coli* F_1F_0–ATPase. (*b*) The rotation of a 3.6-μm-long actin filament in the presence of 5 m*M* MgATP.

Stepwise rotation of the γ subunit of F_1 relative to an immobilized $\alpha_3\beta_3$ unit at low ATP concentration.